Carbohydrate Polymers 79 (2010) 269–276

Contents lists available at ScienceDirect

Carbohydrate Polymers

journal homepage: www.elsevier.com/locate/carbpol

Barrier properties of biodegradable composite films based on kappa-carrageenan/pectin blends and mica flakes

Vítor D. Alves [1], Nuno Costa, Isabel M. Coelhoso *

REQUIMTE/CQFB, Chemistry Department, FCT/Universidade Nova de Lisboa, 2829-516 Caparica, Portugal

ARTICLE INFO

Article history:
Received 9 June 2009
Received in revised form 31 July 2009
Accepted 3 August 2009
Available online 11 August 2009

Keywords:
Barrier properties
Biodegradable films
Kappa-carrageenan
Pectin
Mica flakes

ABSTRACT

In this work, the enhancement of the barrier properties to water vapour and gases (CO_2 and O_2) of a polymeric matrix composed by kappa-carrageenan and pectin (66.7% kappa-carrageenan), with the inclusion of mica flakes, was studied. The effect of the films mica content on the water vapour permeability (WVP) was dependent on the driving force applied. A higher WVP reduction (of about 40% for a mica content of 10%, mass of mica per mass of dry polymer), was observed when the films were more homogenously hydrated throughout their thickness. A significant decrease was also observed for both CO_2 and O_2 permeabilities (73% and 27%, respectively), in conditions where the films were plasticized with water (25% of water, dry basis), for which there is a depletion of the good barrier properties characteristic of dry polysaccharide films. In addition, the composition of 10% of mica flakes in the polymer matrix represented a critical volume fraction of inorganic particles, above which there was a decrease of the films barrier properties, for all components tested.

1. Introduction

With the increasing of consumers concerns on limited natural resources and the environment, the use of renewable resources to produce biodegradable materials that can reduce waste disposal problems, are being explored. Accordingly, a variety of renewable biopolymers have been investigated for the development of biodegradable materials to substitute or complement their non-biodegradable petrochemical-based counterparts (Siracusa, Rocculi, Romani, & Rosa, 2008). Biopolymers, such as polysaccharides (e.g., starch, alginate, pectin, carrageenan, agar, chitosan); proteins (e.g., gluten, gelatine, casein) and their composites (Bertan, Tanada-Palmu, Siani, & Grosso, 2005; Elizondo, Sobral, & Menegalli, 2009; Kayserilioglu, Bakir, Yilmaz, & Akkas, 2003; Lafargue, Lourdin, & Doublier, 2007; Lazaridou & Biliaderis, 2002; López, García, & Zaritzky, 2008; Ma, Yu, & Kennedy, 2005; Wu, Geng, Chang, Yu, & Ma, 2009), which can be obtained from renewable agriculture by-products, food processing industry wastes and natural resources (animals, plants and algae), have been studied. In particular, the recovery of pectins from citrus residues and carrageenans from algae from the Atlantic coast (Hilliou et al., 2006), which are abundant in Portugal, has been investigated.

It was already stated that blends of kappa-carrageenan and pectin are able to form cohesive and transparent films (Alves et al., 2006). Their hydrophilic character has shown to increase with increasing kappa-carrageenan content in the polymer matrix. As such, the water vapour permeability also increased, but reached a plateau at about 67% (dry basis) of kappa-carrageenan. A further increase in the kappa-carrageenan content had not a significant influence on the films water vapour permeability.

Even though films made from polysaccharides are expected to be good oxygen and carbon dioxide barriers due to their tightly packed and ordered hydrogen-bonded network structure, they have poor vapour barrier properties, which result from their hydrophilic nature. In addition, polysaccharide films represent good barrier properties to gases only if they are not plasticized with water or other plasticizers. The gas permeability increases significantly with the increase of the films water/plasticizers content, as observed by Dole, Joly, Espuche, Alric, & Gontard, 2004; Gontard, Thibault, Cuq, & Guilbert, 1996. These facts limit their fields of application, namely in food packaging.

Several strategies have been tested to enhance the water resistance and barrier properties of these films, such as the inclusion of inorganic impermeable particles (Cyras, Manfredi, Ton-That, & Vázquez, 2008; Ray & Bousmina, 2005; Rhim & Ng, 2007); polymer crosslinking (Adoor, Prathab, Manjeshwar, & Aminabhavi, 2007; Da Silva, Bierhalz, & Kieckbusch, 2009; Kolodziejska, Piotrowska, Bulge, & Tylingo, 2006); blends with hydrophobic polymers and lipids (Fabra, Talens, & Chiralt, 2008) and production of

* Corresponding author. Tel.: +351 212948303; fax: +351 212948385.
E-mail address: irc@dq.fct.unl.pt (I.M. Coelhoso).
[1] Present address: CEER – Biosystems Engineering, Instituto Superior de Agronomia, Universidade Técnica de Lisboa, Tapada da Ajuda, 1349-017 Lisboa, Portugal.

0144-8617/$ - see front matter © 2009 Elsevier Ltd. All rights reserved.
doi:10.1016/j.carbpol.2009.08.002

multi-layered films (Elsabee, Abdou, Nagy, & Eweis, 2008; Lee, Son, & Hong, 2008).

In this work, the improvement of the water barrier properties of model composite films based on commercial pectin and kappa-carrageenan, with a kappa-carrageenan content of 67% (dry basis), is investigated, using mica flakes as impermeable barriers. Special attention is driven to study the influence of the water vapour driving force on the water diffusion through the composite films, with different inorganic particles content. In addition, the effect of the mica flakes content on the films permeability to carbon dioxide and oxygen is studied, in conditions where the films are plasticized with water, for which there is a depletion of the good barrier properties that the polysaccharide films possess when dried.

2. Materials and methods

2.1. Films preparation

Commercial kappa-carrageenan and pectin from citrus fruit (Sigma–Aldrich, Spain), and mica flakes (Zemex Industrial Minerals HI Mod270, USA) were used to prepare model carrageenan-pectin-mica aqueous mixtures. The mica particles have an average particle size of 33 μm and an aspect ratio of 10 (manufacturer data sheet). A mass of 0.6 g of dry polymer (66.7% carragenan, mass of carrageenan per mass of dry polymer) and the mica flakes (0%, 5%, 10% and 20%, mass of mica per mass of dry polymer, which corresponds to a flakes volume fraction of 0, 0.026, 0.051 and 0.096, respectively) were dispersed in 2 ml of ethanol to avoid lumping during solution preparation. Water (30 ml) was then added with vigorous stirring. The suspension was heated at 60 °C with constant stirring until a homogeneous solution was obtained. The solution was transferred to a casting container, after the removal of air bubbles from the viscous medium under vacuum. The cast solution was then allowed to dry at 37 °C to form a film. Films thickness was measured at different points using a manual micrometer (Braive Instruments, Belgium).

The mica flakes were exfoliated previously by heating at 800 °C for 2 h and then quenching it in hot saturated aqueous Na_2CO_3 (Barder, 1951). An incomplete exfoliation is expected according to the results obtained by Yang, Smyrl, and Cussler (2004) for PVA-mica films using the same exfoliation procedure and the same mica particles (HiMod 270). Further X-ray Diffraction and Scanning Electron Microscopy studies to characterize the exact particles morphology will be subject of a future publication.

2.2. Water sorption isotherms

Water sorption isotherms were determined by the gravimetric method. Film samples with dimensions of 25 × 25 mm, and mica samples, were previously dried at 60 °C during 48 h. The samples were then placed in desiccators with different relative humidities, imposed by the use of saturated saline solutions. The experiment was carried out at 25 ± 2 °C. The samples were weighed after equilibrated during 1 month. The Guggenheim–Anderson–de Boer (GAB) model (Eq. (1)) was used to fit the experimental sorption data.

$$X = \frac{CkX_0a_w}{[(1-ka_w)(1-ka_w+Cka_w)]} \quad (1)$$

where X is the equilibrium moisture content at the water activity a_w, X_0 is the monolayer moisture content and represents the water content corresponding to saturation of all primary adsorption sites by one water molecule, C is the Guggenheim constant and represents the energy difference between the water molecules attached to primary sorption sites and those absorbed to successive sorption layers, and k is the corrective constant taking into account properties of multilayer molecules with respect to the bulk liquid. GAB equation parameters were calculated by non-linear fitting using the software package Scientist™, from MicroMath®.

2.3. Water vapour permeability

The water vapour permeability was measured gravimetrically. The films were sealed with silicone to the top of a glass petri dish with a diameter of 5 cm. Two different driving forces were imposed. In the first one, pure water was used inside the petri dish (RH = 100%) placed in a desiccator containing drierite (RH = 10.8%). The water vapour permeability was measured using films conditioned previously at a relative humidity of 94%. The second driving force tested was imposed using a saturated sodium chloride solution (RH = 75.4%) inside the petri dish and a saturated sodium nitrite solution outside (RH = 60.5%), and the films tested were previously equilibrated at a relative humidity of 75%. A fan was used to promote the circulation of air inside the desiccator, in order to minimize the mass transfer resistance of the air boundary layer above the membrane. The room temperature and the relative humidity outside the petri dish were measured over time using a thermohygrometer (Vaisala, Finland). The water vapour flux was determined by weighing the petri dish in regular time intervals for 2–3 days.

2.4. Gas permeability

The experimental apparatus used is composed of a stainless steel cell with two identical chambers separated by the test film. The films were previously equilibrated at a constant relative humidity in order to possess a water content of 25% (dry basis) in the beginning of each experiment. The permeability was evaluated by pressurizing one of the chambers (feed) up to 1.0 bar, with pure carbon dioxide or oxygen followed by the measurement of the pressure change in both chambers over time, using two pressure transducers (Druck, PDCR 910 model, England, for the feed chamber, and a Baratron Pressure Sensor, model 627B, USA, for the permeate chamber). The measurements were made at constant temperature, 30 °C, using a thermostatic bath (Julabo, Model EH, Germany). High-purity grade carbon dioxide (99.998%) and oxygen (99.999%), Praxair, Spain, were used. The permeability was calculated with the pressure data obtained from both compartments according to the following equation (Wang, DeRocher, Wu, Bates, & Cussler, 2006):

$$\frac{1}{\beta}\ln\left(\frac{[p_f-p_p]_0}{[p_f-p_p]}\right) = \frac{1}{\beta}\ln\left(\frac{\Delta p_0}{\Delta p}\right) = P\frac{t}{\delta} \quad (2)$$

where p_f and p_p are the pressures in the feed and permeate compartments, respectively; P is the gas permeability; t is the time; and δ is the film thickness. The geometric parameter β is $A(1/V_f + 1/V_p)$, where V_f and V_p are the volumes of the feed and permeate compartments, respectively, and A is the membrane area. This parameter was calculated ($\beta = 112.9\ m^{-1}$) with a PDMS membrane and nitrogen as test gas, using the permeability value referred in the literature, $P_{N_2/PDMS} = 9.7 \times 10^{-14}$ mol m/m^2 s Pa (Houston, Weinkauf, & Stewart, 2002). The film sample gas permeability is equal to the slope obtained representing $\ln(\Delta p_0/\Delta p)$ as a function of $\beta t/\delta$.

2.5. Scanning Electron Microscopy

The films cross sections were observed by a ZEISS 960 scanning electron microscope. The samples were fixed by mutual conductive adhesive tape on aluminum stubs and covered with gold palladium using a sputter coater.

3. Results and discussion

The films prepared were flexible and resistant when handled, with a thickness of 55.1 ± 6.8 μm. Without mica flakes, they were completely transparent, however, with the inclusion of mica they became less transparent but translucid. In Fig. 1 are presented Scanning Electron Microscopy (SEM) pictures of the films cross section. It can be observed that the internal morphology changed dramatically as more mica flakes were added to the polymeric matrix. It became more heterogeneous, especially for 20% mica content.

The effect of the mica content on the water vapour and gas transport through the polymeric matrix, was studied. The water vapour transport was evaluated applying two different driving forces: 100.0–10.8 %RH and 75.4–60.5 %RH. Regarding the gas transport study, all the process parameters were maintained constant (driving force, temperature and water content of the film), except the mica/polymer proportion.

3.1. Water sorption isotherms

Water sorption isotherms of the film samples obtained for the carrageenan/pectin mixture (67% carrageenan), varying the content of mica flakes (0%, 5%, 10% and 20%), are presented in Fig. 2 together with the GAB model fitted for each film and the respective parameters. The GAB model fitted reasonably well the experimental results. For all film samples the curve presents a sigmoidal shape and the equilibrium moisture content increases slowly with increasing environmental a_w up to 0.6, beyond which a steep rise in moisture content is observed.

It can also be seen that the amount of moisture adsorbed per mass of dry solids by the sample films is not depend on the mica content, even though there is a decrease of the polymer proportion (mass of polymer per mass of dry solids) as the mica content increases. This fact may be explained by the water sorption capacity of the mica flakes themselves (Fig. 2). In fact, when separated from the polymer matrix, mica flakes have shown this capacity, which was especially high for water activities above 0.75. However, the adsorption behaviour of the films is not the sum of that of both solids separately. Both are contributing, but differently, when compared to their behaviour when isolated, possibly due to interactions between the three components involved (water, polymers and flakes) and alterations on the morphology of the polymer matrix. This results in a similar water sorption ability of the films with different mica contents.

3.2. Water flux

The measured water flux for the different experimental conditions is presented in Fig. 3. The relative values obtained are in accordance with the driving forces imposed, since higher values

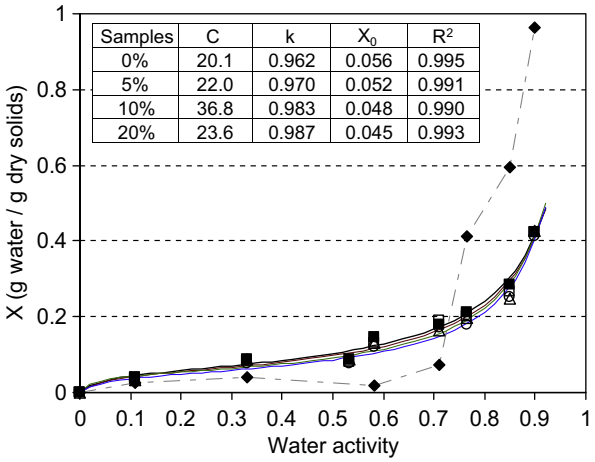

Fig. 2. Experimental moisture sorption isotherms of kappa-carrageenan/pectin films with different amounts of mica flakes: (■) 0% , (□) 5%, (△) 10% and (○) 20% (mass of mica per mass of dry polymer); the respective fitted GAB curves (lines) and GAB parameters (inserted table). The sorption isotherm of isolated mica flakes is also presented (♦).

were achieved for the higher driving force. It also can be seen that, for the higher driving force, the water flux decreases about 15% with the inclusion of 5% of mica flakes, but for mica contents above 5%, it remained practically constant. On the other hand, the flux seemed to be not affected by the mica content when the lower driving force was used. These results alone are not sufficient to evaluate the effect of the mica content on the films barrier properties, since the water flux is highly dependent, not only on the driving force and on the film characteristics, but also on the mass transfer rate in the boundary layer adjoining the test film.

3.3. Water vapour permeability and diffusion coefficients

3.3.1. Water vapour permeability

The water transport in the experimental set-up used involves the following steps (Fig. 4): (i) evaporation at the solution interface inside the petri dish, (ii) diffusion through the stagnant film of air below the test film, (iii) water adsorption at the film interface inside the petri dish, (iv) water diffusion through the test film and (v) water desorption at the film's interface outside the petri dish. In this work, the resistance to water transfer in the boundary layer above the film was neglected, since a fan was used to promote favourable hydrodynamic conditions inside the desiccator.

The water vapour permeability (WVP) was calculated using Eq. (3).

$$\mathrm{WVP} = \frac{N_w \times \delta}{\Delta P_{w,eff}} \tag{3}$$

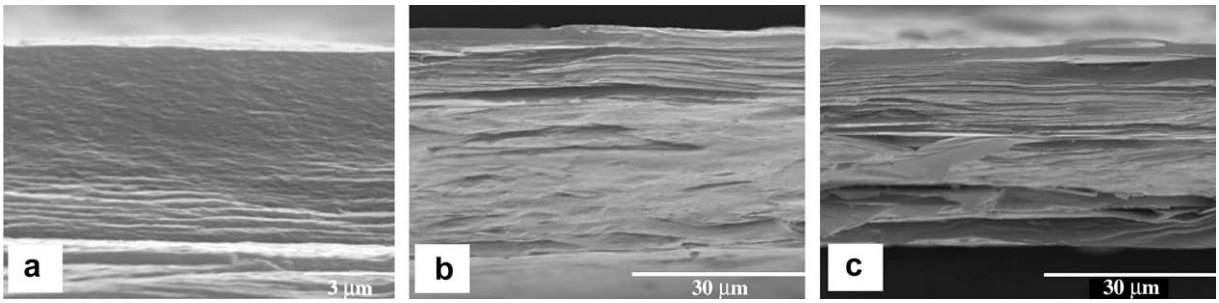

Fig. 1. Scanning Electron Microscopy pictures of the films cross section: (a) 5% mica, (b) 10% mica, (c) 20% mica.

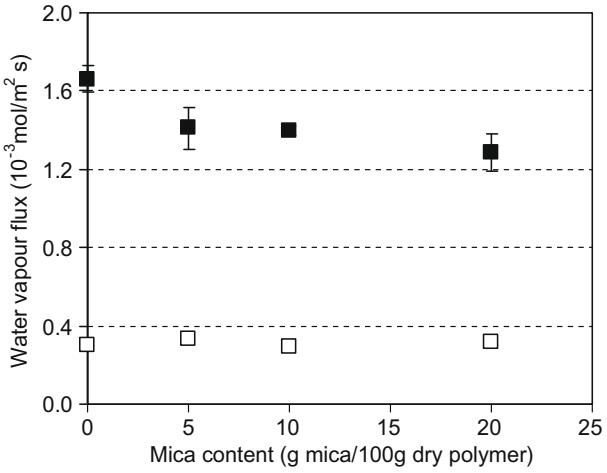

Fig. 3. Water vapour flux as a function of mica content for two driving forces: 100.0–10.8 %RH (filled symbols) and 75.4–60.5 %RH (opened symbols).

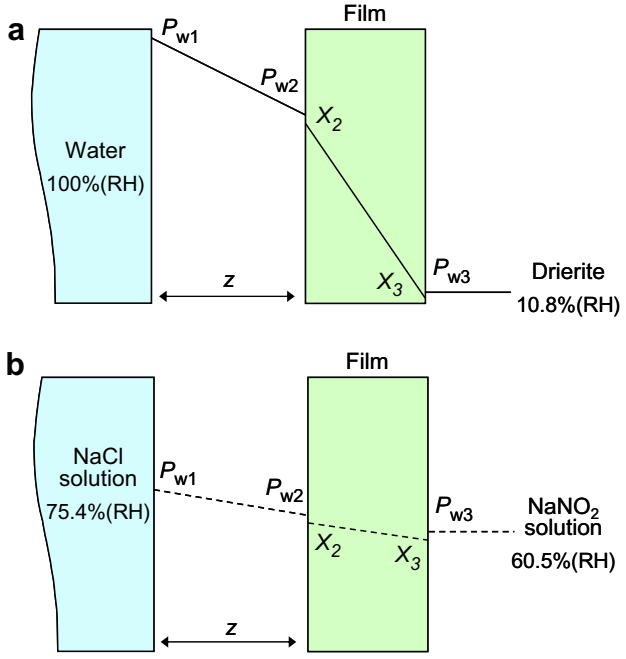

Fig. 4. Water vapour pressure profiles on the films boundary layers and water concentration inside the films for both driving forces: (a) 100.0–10.8 %RH and (b) 75.4–60.5 %RH.

In which, N_w is the water vapour molar flux, δ is the film thickness and $\Delta P_{w,eff}$ is the effective driving force, expressed as the water vapour pressure difference between both sides of the film, calculated taking into account the mass transfer resistance of the stagnant film of air below the test film, and is given by:

$$\Delta P_{w,eff} = P_{w2} - P_{w3} \quad (4)$$

The unknown value of P_{w2} was determined using Eq. (5), taking into account that, at steady state conditions, the measured water flux (N_w) is equal to the flux through the stagnant film of air that separates the surface of the liquid from the surface of the test film:

$$N_w = \frac{P}{RTz} D_{w-air} \ln\left(\frac{P - P_{w2}}{P - P_{w1}}\right) \quad (5)$$

where P is the atmospheric pressure, R the gas constant, T the temperature, z the distance from the test film to the solution's surface, D_{w-air} the water vapour diffusion coefficient in air, P_{wi} is the water partial pressure contacting the liquid surface and the test film ($P_{wi} = a_{wi} \times P^*_w$). The value of P_{w1} is known, and was calculated with the water activity of the liquid phase (a_{w1}) and the pure water vapour pressure (P^*_w). The water partial pressure outside de petri dish (P_{w3}) was calculated using the measured %RH values ($P_{w3} = a_{w3}P^*_w = \%RH \times P^*_w/100$). The obtained values for $\Delta P_{w,eff}$ were 2150 ± 143 and 237 ± 48 Pa, for the experiments using the relative humidity differences 100.0–10.8% and 75.4–60.5%, respectively, at ambient temperature (T = 25 ± 2 °C).

The WVP results are presented in Fig. 5. As can be observed, the water vapour permeability is higher when the driving force 75.4–60.5 (%RH) was applied, for all mica contents studied. This fact is related to the hydrophilic character of the films material, expressed by the water sorption isotherms. The water entering the films is acting as a diffusion species and also as a plasticizer. In this way, it loosens the polymeric matrix and, consequently, water transport is facilitated.

When the 75.4–60.5 (%RH) difference was used, both film surfaces where in contact with a relatively high water activity. As a result, the film is hydrated throughout the entire water diffusion path. On the contrary, when the 100–10.8 (%RH) driving force is applied, even though one of the surfaces is in contact with an atmosphere with a high water activity, the other surface is exposed to an almost dry environment (Fig. 4). Therefore, there is a high water concentration gradient through the film thickness, limiting the plasticizing effect, and part of the polymeric matrix maintains its tightly packed network structure which contributes to hinder water transport. A similar behaviour was obtained by Mauer, Smith, & Labuza, 2000, with β-casein films tested using two driving forces: 53–11 (%RH) and 76–53 (%RH). A higher WVP was observed with the later driving force (2.9×10^{-11} mol m/m^2 s Pa) when compared to that measured with the 53–11 %RH difference (1.0×10^{-11} mol m/m^2 s Pa).

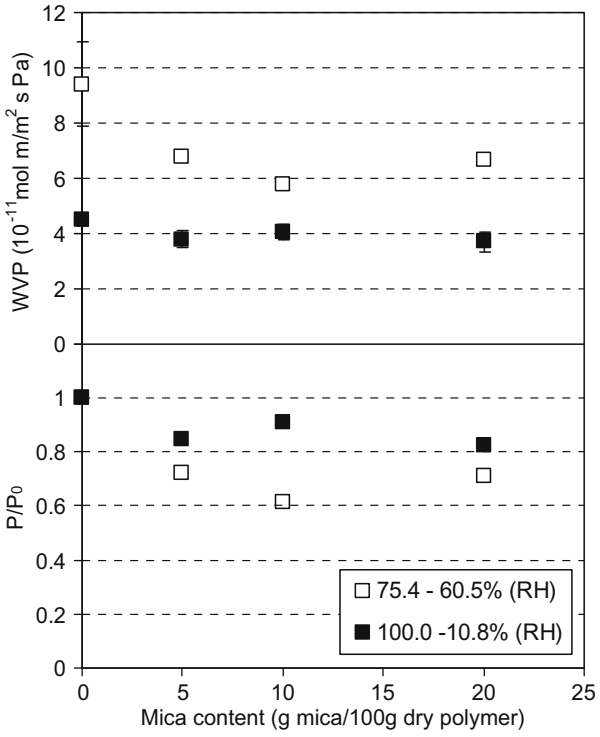

Fig. 5. Water vapour permeability as a function of mica content. P/P_0 represents the normalized WVP values.

The WVP values of the films without mica flakes are in the same order of magnitude of that referred for films from other biopolymers, namely from starch, in the ranges of 1.4–4.4 $\times 10^{-11}$ mol m/m^2 s Pa (Bertuzzi, Vidaurre, Armada, & Gottifredi, 2007) and 3.7–4.6 $\times 10^{-11}$ mol m/m^2 s Pa (Mali, Grossmann, García, Martino, & Zaritzky, 2006), and fish gelatin (5.6 $\times 10^{-11}$ mol m/m^2 s Pa) (Sztuka & Kolodziejska, 2009), but higher than that presented for chitosan (8.5 $\times 10^{-12}$ mol m/m^2 s Pa) (Srinivasa, Ramesh, & Tharanathan, 2007). However, a comparison of results from different authors is rather difficult, as the WVP is highly dependent not only on the driving force applied, but also on the films thickness and on the correction method used to quantify the mass transfer resistance of the stagnant air below the film.

Regarding the effect of mica flakes content on the water vapour permeability, two different behaviours were observed (Fig. 5). Although for both driving forces the permeability decreased about 20% for a mica content of 5%, those tested with the higher driving force seemed to be no further affected by the inclusion of more mica flakes in the polymeric matrix. On the other hand, for the lower driving force, the water permeability reached a minimum at a mica content of 10%, with a value of about 60% of the initial value, increasing again with the inclusion of 20% mica to a value close to that obtained for the higher driving force. This fact may be related to the different water content of the films, which altered in different ways the internal films morphology and the diffusion path of the water molecules.

The permeability may be expressed as the product of the water sorption coefficient (S) to the effective water diffusion coefficient (D_{eff}). In the case of the films studied, according to the water sorption isotherms (Fig. 2), the sorption coefficient is expected to be pretty similar for all the films tested, at a given water activity. In this way, the major contribution for the differences encountered in the water vapour permeability values, when the mica content was changed for the same driving force, should be attributed to a variation of the effective diffusion coefficient. The determination of D_{eff} and S is carried out in the next section.

3.3.2. Water diffusion coefficients

The molar water flux (N_w) through the test film at steady-state may be expressed using Eq. (6), which is based on the first Fick's Law:

$$N_W = \frac{D_{eff}\rho_s}{M_w}\frac{X_2 - X_3}{\delta} \quad (6)$$

In which ρ_s is the dry film density, M_w is the water molar mass, X_i is the water concentration (mass of water/mass of dry polymer) in both film interfaces ($X_2 > X_3$) and δ is the film thickness (Fig. 4). At equilibrium, the X_i values may be related to the water activity using the water sorption isotherms by Eq. (7) (Larotonda, Matsui, Sobral, & Laurindo, 2005):

$$S_i^* = \tan(\theta) = \frac{X_i}{a_{wi}} \quad (7)$$

where S_i^* [g_{water}/g_{solids}] is the water sorption coefficient of the film material, which can be converted to S_i [g_{water}/g_{solids} Pa] by dividing Eq. (7) by the pure water vapour pressure:

$$S_i = \frac{X_i}{a_{wi}P_w^*} \quad (8)$$

Combining Eqs. (6) and (8), an expression which enables the determination of the effective diffusion coefficient is obtained:

$$D_{eff} = \frac{N_W M_w}{\rho_s P_w^*(S_2 a_{w2} - S_3 a_{w3})} \quad (9)$$

The values obtained are presented in Fig. 6, and the calculated sorption coefficients are shown in Table 1.

It can be seen that, as expected, the later do not change significantly with the increase of mica content for each driving force applied, but diverge when comparing different driving forces. Regarding the effective diffusion coefficient values, they follow the same trend of that of the water vapour permeability presented in Fig. 5, for both driving forces studied. From this fact we can conclude that, for each driving force, the change in the water permeability is essentially due to a variation of the effective diffusion coefficient due to the presence of the mica flakes. However, when comparing different driving forces, the water vapour permeability is dependent on both S and D_{eff}. A higher S value means a higher water concentration in the polymer, which has a positive impact on D_{eff}. In fact, that is what happens when the 75.4–60.5 %RH driving force is used. The film is more hydrated and plasticized throughout all its thickness (even though the %RH difference is low), which turns the polymeric matrix less compact resulting in a much higher effective diffusion coefficients, for all mica contents.

3.4. Gas permeability

The measured permeability to carbon dioxide and oxygen as a function of the mica content is presented in Fig. 7. The values ob-

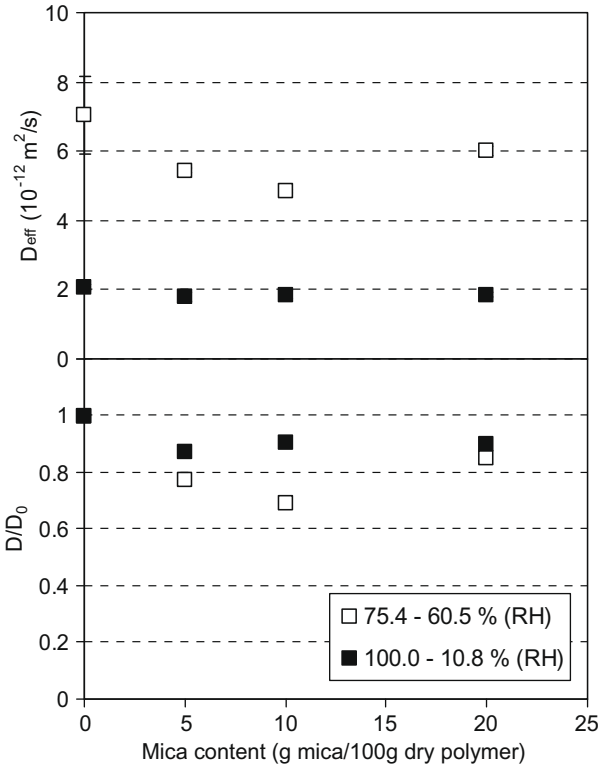

Fig. 6. Effective diffusion coefficient of water through the films as a function of mica content. D/D_0 represents the normalized D_{eff} values.

Table 1
Water sorption coefficients in both sides of the films for the driving forces studied (the errors associated to the S values are below 5.2%).

ΔRH (%)	Mica content							
	0%		5%		10%		20%	
	S_2	S_3	S_2	S_3	S_2	S_3	S_2	S_3
100.0–10.8	18.9	3.9	18.6	3.6	19.7	2.7	20.7	2.9
75.4–60.5	12.6	12.6	10.9	10.9	10.5	10.5	10.4	10.4

tained for carbon dioxide and oxygen are four and six orders of magnitude lower than that of water vapour, respectively. It can be observed a large reduction of the permeability to carbon dioxide, of about 73%, for a mica content of 10%, after which it increased when a mica content of 20% was used. The oxygen permeability observed is one hundred times lower than that of carbon dioxide. This fact may be related to its poor interaction with the hydrated film with 25% of water (dry basis), taking into account the relative solubilities of oxygen (0.037 g O_2/kg H_2O) and carbon dioxide (1.30 g CO_2/kg H_2O) in water at 1 atm and 30 °C (Dean & A., 1978). However, further studies are needed to determine the solubility of both components in the films.

For oxygen, the polymeric matrix itself represents already a very good barrier, but the barrier properties are further enhanced with the inclusion of mica flakes, for the conditions tested. There is a decrease of the permeability of about 27% for a mica content of 10%, after which it rises again. In fact, a similar trend was detected for the water vapour permeability, when the 75.4–60.5 %RH driving force was applied, and for the CO_2 permeability. The permeability reaches a minimum for a critical mica content of 10% mica flakes, and a higher amount of flakes on the polymeric matrix has a negative impact on the barrier properties. This behaviour seems to be related to the hydration degree throughout the films thickness, since for the case of water vapour, it occurs only when the water in the films is more homogeneously distributed through the diffusion path.

The CO_2 and O_2 permeability of hydrophilic films, namely from polysaccharides, are extremely dependent on its water content, as observed by Gontard et al. (1996) for wheat gluten films. These authors presented an increase of the oxygen permeability of about 950 times for a change of the films water content from 7.5% to 42% (dry basis); and an increase of nearly 36,550 times on the CO_2 permeability, for a variation of the relative humidity of the atmosphere in contact with the film from 60% to 95%. Thus, it is difficult the comparison of results presented by different authors, unless the exact films water content for each study is specified. The O_2 and CO_2 permeabilities referred by Gontard et al. (1996) for wheat gluten films (26×10^{-17} and 16×10^{-15} mol m/m^2 s Pa, respectively), with a similar water content of that of the films studied in this work, is above of that of kappa-carrageenan/pectin films without flakes (4.0×10^{-17} and 3.9×10^{-15} mol m/m^2 s Pa, respectively). Cerqueira, Lima, Teixeira, Moreira, and Vicente, (2009), characterized edible coatings based on novel galactomannans and glycerol as plasticizer. They presented values for CO_2 and O_2 permeabilities in the ranges of $0.7–1.4 \times 10^{-15}$ mol m/m^2 s Pa and $1.0–3.1 \times 10^{-17}$ mol m/m^2 s Pa, respectively. These values are close to that presented in this work; however the authors did not indicate the water content of the films.

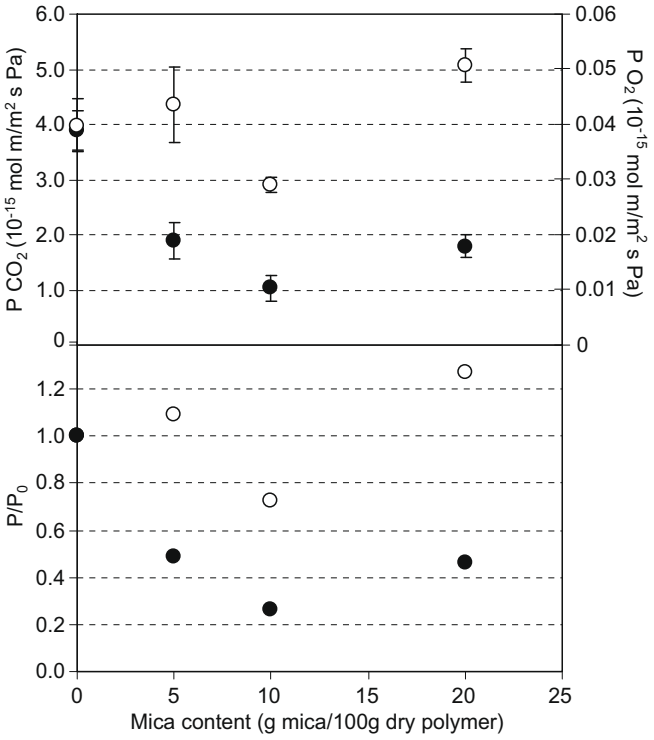

Fig. 7. Carbon dioxide permeability (filled symbols) and oxygen permeability (opened symbols), as a function of mica content. P/P_0 represents the normalized P_{CO_2} and P_{O_2} values.

If we compare the gas barrier properties obtained in this work to that referred for synthetic polymers, we conclude that the kappa-carrageenan/pectin/mica flakes matrix, even plasticized with 25% (dry basis) of water, has a much lower oxygen permeability ($P(O_2) \leqslant 4.3 \times 10^{-17}$ mol m/m^2 s Pa) than the values presented for LDPE ($P(O_2) = 1.0 \times 10^{-15}$ mol m/m^2 s Pa, Gontard et al., 1996), HDPE ($P(O_2) = 2.0 \times 10^{-16}$ mol m/m^2 s Pa, Miller & Krochta, 1997) and PP ($P(O_2) = 2.6 \times 10^{-16}$ mol m/m^2 s Pa, Costamagna, Strumia, López-González, & Riande, 2007). Regarding carbon dioxide, the inclusion of a mica content of 10% on the kappa-carrageenan/pectin matrix plasticized with 25% (dry basis) of water ($P(CO_2) = 1.0 \times 10^{-15}$ mol m/m^2 s Pa), enabled to reach higher barrier properties than LDPE ($P(CO_2) = 4.2 \times 10^{-15}$ mol m/m^2 s Pa, Gontard et al., 1996) and a similar value to that observed for PP ($P(CO_2) = 0.9 \times 10^{-15}$ mol m/m^2 s Pa, Costamagna et al., 2007).

In what concerns the effect of the mica flakes loading on water vapour and gas permeability, we would expect a continuous decrease of these parameters as more mica flakes were included in the polymer matrix, since they constitute impermeable barriers and would increase the diffusion path of the permeants. In fact, these were the results presented by Yang et al. (2004) for the permeation of HCl through a PVA film containing the same mica flakes used in this work. However, their experimental conditions were completely different from those used in this work, involving the swelling of the films in water before the experiments and the use of a different polymer, which results on the creation of a different polymer matrix in terms of composition and morphology. A similar trend on permeability reduction was presented in the work of Picard, Vermogen, Gérard, & Espuche, 2007, on the permeation of water and gases (H_2, He and O_2) through polyamide films with increasing montmorillonite nanoclay content. In this case, the different trend may also be explained by the different polymer matrix, which is much less hygroscopic than the polymers used in this work.

On the other hand, Bharadwaj et al., 2002 observed a decrease of O_2 permeability through polyester-clay nanocomposites until a critical nanoclay content, after which an increase of permeability was detected. These results are in agreement to that presented in this work. They explained this behaviour with a lack of nanoclay exfoliation or decrease of aspect ratios, which means that the particles were not in the nanometer range, possibly in the micrometer range, as those used in the present work.

When inorganic particles are included in a polymer matrix, their effect on the composite permeability is closely related to the type of interaction of the particles with the permeant species, as well as with the polymer and the resulting internal morphology. In this work, the water adsorbs not only to the polymer, but also to the mica flakes. The swelling of both solids may create zones around the particles were the diffusion is higher. After a certain mica content, the increase of the diffusion path due to the impermeable barriers is compensated by the contribution of the higher diffusion zones, leading to a constant or even to an increase of the permeability.

The increase of gas permeability in polymer-inorganic composites was also referred in various works, namely with nano-composite membranes, some reviewed by Cong and co-workers (Cong, Radosz, Towler, & Shen, 2007). The increase of gas permeability with the inclusion of inorganic particles was explained by either an increase of the free volume (Higuchi et al., 2000; Merkel et al., 2003; Winberg et al., 2005), by a poor interaction polymer-nanoparticle with the creation of nano-gaps around the particles (Cong et al., 2007) or by a strong interaction of the diffusing molecules with the particles (Kim, Ha, & Lee, 2001).

4. Conclusions

In this work, the effect of the inclusion of mica flakes on the barrier properties of a polymeric matrix composed by kappa-carrageenan and pectin (66.7% kappa-carrageenan), was evaluated. The enhancement of the barrier properties to water vapour was dependent on the driving force applied. Although for both driving forces tested the permeability decreased about 20% for a mica content of 5%, when the higher driving force was applied (100–10.8 %RH), the WVP seemed to be no further affected by the inclusion of more mica flakes. On the contrary, for the lower driving force (75.4–60.5 %RH), for which the films were homogenously hydrated throughout all their thickness, the water permeability reached a minimum at a mica content of 10%, with a value of about 60% of the initial value. In addition, it was confirmed that, for each driving force, similar water sorption coefficients were observed for all mica contents, and the reduction of the WVP was essentially due to a decrease of the effective water diffusion coefficient.

Regarding the barrier properties to gases, a significant decrease of the permeability was observed for both CO_2 and O_2 (73% and 27%, respectively), in relation to the films without mica flakes. These results are interesting, since it was possible to increase the barrier properties to CO_2 and O_2 of hydrated films (with 25% of water, dry basis), in conditions for which the polysaccharide films start to loose the good gas barrier properties that they possess when dried. Furthermore, it was observed that the composition of 10% of mica flakes in the polymer matrix represents a critical volume fraction of these inorganic particles, above which there is a decrease of the films barrier properties, for all components tested.

Acknowledgements

Vítor D. Alves acknowledges Fundação para a Ciência e a Tecnologia, Pos-doc fellowship SFRH/BPD/26178/2005. The financial support from Fundação para a Ciência e a Tecnologia within the Project POCTI/EQU/45595/2002 is also acknowledged.

References

Adoor, S. G., Prathab, B., Manjeshwar, L. S., & Aminabhavi, T. M. (2007). Mixed matrix membranes of sodium alginate and poly(vinyl alcohol) for pervaporation dehydration of isopropanol at different temperatures. *Polymer, 48*(18), 5417–5430.

Alves, V., Costa, N., Hilliou, L., Larotonda, F., Gonçalves, M., Sereno, A., et al. (2006). Design of biodegradable composite films for food packaging. *Desalination, 199*, 331–333.

Barder, J. J. (1951). Methods for treating mica and composition, *US Patent Office*, Patent no. 2 549 880.

Bertan, L. C., Tanada-Palmu, P. S., Siani, A. C., & Grosso, C. R. F. (2005). Effect of fatty acids and "Brasilian elemi" on composite films based on gelatine. *Food Hydrocolloids, 19*, 73–82.

Bertuzzi, M. A., Vidaurre, E. F. C., Armada, M., & Gottifredi, J. C. (2007). Water vapor permeability of edible starch based films. *Journal of Food Engineering, 80*, 972–978.

Cerqueira, M. A., Lima, A. M., Teixeira, J. A., Moreira, R. A., & Vicente, A. A. (2009). Suitability of novel galactomannans as edible coatings for tropical fruits. *Journal of Food Engineering, 94*, 372–378.

Cong, H., Radosz, M., Towler, B. F., & Shen, Y. (2007). Polymer-inorganic nanocomposite membranes for gas separation. *Separation and Purification Technology, 55*, 281–291.

Costamagna, V., Strumia, M., López-González, M., & Riande, E. (2007). Gas transport in surface grafted polypropylene films with poly(acrylic acid) chains. *Journal of Polymer Science Part B: Polymer Physics, 45*(17), 2421–2431.

Cyras, V. P., Manfredi, L. B., Ton-That, M. T., & Vázquez, A. (2008). Physical and mechanical properties of thermoplastic starch/montmorillonite nanocomposite films. *Carbohydrate Polymers, 73*, 55–63.

Da Silva, M. A., Bierhalz, A. C. K., & Kieckbusch, T. G. (2009). Alginate and pectin composite films crosslinked with Ca^{2+} ions: Effect of the plasticizer concentration. *Carbohydrate Polymers, 77*, 736–742.

Dean, J. A. (1978). *Lange's handbook of chemistry*. New York: McGraw-Hill Book Company.

Dole, P., Joly, C., Espuche, E., Alric, I., & Gontard, N. (2004). Gas transport properties of starch based films. *Carbohydrate Polymers, 58*, 335–343.

Elizondo, N. J., Sobral, P. J. A., & Menegalli, F. C. (2009). Development of films based on blends of *Amaranthus cruentus* flour and poly(vinyl alcohol). *Carbohydrate Polymers, 75*, 592–598.

Elsabee, M. Z., Abdou, E. S., Nagy, K. S. A., & Eweis, M. (2008). Surface modification of polypropylene films by chitosan and chitosan/pectin multilayer. *Carbohydrate Polymers, 71*, 187–195.

Fabra, M. J., Talens, P., & Chiralt, A. (2008). Effect of alginate and λ-carrageenan on tensile properties and water vapour permeability of sodium caseinate-lipid based films. *Carbohydrate Polymers, 74*, 419–426.

Gontard, N., Thibault, R., Cuq, B., & Guilbert, S. (1996). Influence of relative humidity and film composition on oxygen and carbon dioxide permeabilities of edible films. *Journal Agricultural and Food Chemistry, 44*, 1064–1069.

Higuchi, A., Agatsuma, T., Uemiya, S., Kojima, T., Mizoguchi, K., Pinnau, I., et al. (2000). Preparation and gas permeation of immobilized fullerene membranes. *Journal of Applied Polymer Science, 7*, 529–537.

Hilliou, L., Larotonda, F. D. S., Abreu, P., Ramos, A. M., Sereno, A. M., & Gonçalves, M. P. (2006). Effect of extraction parameters on the chemical structure and gel properties of κ/ι-hybrid carrageenans obtained from Mastocarpus stellatus. *Biomolecular Engineering, 23*(4), 201–208.

Houston, K. S., Weinkauf, D. H., & Stewart, F. F. (2002). Gas transport characteristics of plasma treated poly(dimethylsiloxane) and polyphosphazene membrane materials. *Journal of Membrane Science, 205*, 103–112.

Kayserilioglu, B. S., Bakir, U., Yilmaz, L., & Akkas, N. (2003). Use of xylan, an agricultural by-product, in wheat gluten based biodegradable films: Mechanical, solubility and water vapour transfer rate properties. *Bioresource Technology, 87*, 239–246.

Kim, J. H., Ha, S. Y., & Lee, I. M. (2001). Gas permeation of poly(amide-6-b-ethylene oxide) copolymer. *Journal of Membrane Science, 190*, 179–193.

Kolodziejska, I., Piotrowska, B., Bulge, M., & Tylingo, R. (2006). Effect of transglutaminase and 1-ethyl-3-(3-dimethylaminopropyl) carbodiimide on solubility of fish gelatine-chitosan films. *Carbohydrate Polymers, 65*, 404–409.

Lafargue, D., Lourdin, D., & Doublier, J. L. (2007). Film-forming properties of a modified starch/k-carrageenan mixture in relation to its rheological behaviour. *Carbohydrate Polymers, 70*, 101–111.

Larotonda, F. D. S., Matsui, K. N., Sobral, P. J. A., & Laurindo, J. B. (2005). Hygroscopicity and water vapor permeability of Kraft paper impregnated with starch acetate. *Journal of Food Engineering, 71*, 394–402.

Lazaridou, A., & Biliaderis, C. G. (2002). Thermophysical properties of chitosan, chitosan–starch and chitosan–pollulan films near the glass transition. *Carbohydrate Polymers, 48*, 179–190.

Lee, J. W., Son, S. M., & Hong, S. I. (2008). Characterization of protein-coated polypropylene films as a novel composite structure for active food packaging application. *Journal of Food Engineering, 86*, 484–493.

López, O. V., García, M. A., & Zaritzky, N. E. (2008). Film forming capacity of chemically modified corn starches. *Carbohydrate Polymers, 73*, 573–581.

Ma, X., Yu, J., & Kennedy, J. F. (2005). Studies on the properties of natural fibers-reinforced thermoplastic starch composites. *Carbohydrate Polymers, 62*(1), 19–24.

Mali, S., Grossmann, M. V. E., García, M. A., Martino, M. N., & Zaritzky, N. E. (2006). Effects of controlled storage on thermal, mechanical and barrier properties of plasticized films from different starch sources. *Journal of Food Engineering, 75*, 453–460.

Mauer, L. J., Smith, D. E., & Labuza, T. P. (2000). Water vapor permeability, mechanical, and structural properties of edible β-casein films. *International Dairy Journal, 10*(5–6), 353–358.

Merkel, T. C., He, Z., Pinnau, I., Freeman, B. D., Hill, A. J., & Meakin, P. (2003). Sorption and transport in poly(2, 2-bis(trifluoromethyl)-4, 5-difluoro-1, 3-dioxole-co-tetrafluoroethylene) containing nanoscale fumed silica. *Macromolecules, 36*, 8406–8484.

Miller, K. S., & Krochta, J. M. (1997). Oxygen and aroma barrier properties of edible films: A review. *Trends in Food Science & Technology, 8*, 228–237.

Picard, E., Vermogen, A., Gérard, J. F., & Espuche, E. (2007). Barrier properties of nylon 6-montmorillonite nanocomposite membranes prepared by melt blending: Influence of the clay content and dispersion state consequences on modelling. *Journal of Membrane Science, 292*, 133–144.

Ray, S. S., & Bousmina, M. (2005). Biodegradable polymers and their layered silicate nanocomposites: In greening the 21st century materials world. *Biomolecular Engineering, 23*(4), 962–1079.

Rhim, W., & Ng, P. K. W. (2007). Natural biopolymer-based nanocomposite films for packaging applications. *Critical Reviews in Food Science and Nutrition, 47*(4), 411–433.

Siracusa, V., Rocculi, P., Romani, S., & Rosa, M. D. (2008). Biodegradable polymers for food packaging: A review. *Trends in Food Science & Technology, 19*, 634–643.

Srinivasa, P. C., Ramesh, M. N., & Tharanathan, R. N. (2007). Effect of plasticizers and fatty acids on mechanical and permeability characteristics of chitosan films. *Food Hydrocolloids, 21*(7), 1113–1122.

Sztuka, K., & Kolodziejska, I. (2009). The influence of hydrophobic substances on water vapour permeability of fish gelatin films modified with transglutaminase or 1-ethyl-3-(3-dimethylaminopropyl) carbodiimide (EDC). *Food Hydrocolloids, 23*, 1062–1064.

Wang, J., DeRocher, J. P., Wu, L., Bates, F. S., & Cussler, E. L. (2006). Barrier films made with various lamellar block copolymers. *Journal of Membrane Science, 270*, 12–21.

Winberg, P., DeSitter, K., Dotremont, C., Mullens, S., Vankelecom, I. F. J., & Maurer, F. H. J. (2005). Free volume and interstitial mesopores in silica filled poly(1-trimethylsilyl-1-propyen) nanocomposites. *Macromolecules, 38*, 3776–3782.

Wu, Y., Geng, F., Chang, P. R., Yu, J., & Ma, X. (2009). Effect of agar on the microstructure and performance of potato starch film. *Carbohydrate Polymers, 76*, 299–304.

Yang, C., Smyrl, W. H., & Cussler, E. L. (2004). Flake alignment in composite coatings. *Journal of Membrane Science, 231*, 1–12.